Two-Dimensional Diffusion of Amphiphiles in Phospholipid Monolayers at the Air-Water Interface

Frank Caruso,* Franz Grieser,* Peter J. Thistlethwaite,* and Mats Almgren‡
*School of Chemistry, University of Melbourne, Parkville 3052, Australia, and ‡Department of Physical Chemistry, University of Uppsala, S-751 21, Uppsala, Sweden

ABSTRACT Steady-state and time-resolved fluorescence spectroscopy has been used to examine lateral diffusion in dipalmitoyl-L-α-phosphatidylcholine (DPPC) and dimyristoyl-L-α-phosphatidylcholine (DMPC) monolayers at the air-water interface, by studying the fluorescence quenching of a pyrene-labeled phospholipid (pyrene-DPPE) by two amphiphilic quenchers. Steady-state fluorescence measurements revealed pyrene-DPPE to be homogeneously distributed in the DMPC lipid matrix for all measured surface pressures and only in the liquid-expanded (LE) phase of the DPPC monolayer. Time-resolved fluorescence decays for pyrene-DPPE in DMPC and DPPC (LE phase) in the absence of quencher were best described by a single-exponential function, also suggesting a homogeneous distribution of pyrene-DPPE within the monolayer films. Addition of quencher to the monolayer film produced nonexponential decay behavior, which is adequately described by the continuum theory of diffusion-controlled quenching in a two-dimensional environment. Steady-state fluorescence measurements yielded lateral diffusion coefficients significantly larger than those obtained from time-resolved data. The difference in these values was ascribed to the influence of static quenching in the case of the steady-state measurements. The lateral diffusion coefficients obtained in the DMPC monolayers were found to decrease with increasing surface pressure, reflecting a decrease in monolayer fluidity with compression.

INTRODUCTION

Biomembranes are composed mainly of a lipid bilayer in which the membrane proteins and carbohydrates are embedded. In many cases, the lipids and proteins are able to undergo lateral and rotational diffusion within the lipid matrix (Chapman, 1993). Fluidity constitutes an important membrane characteristic, as it seems to play a significant role in modulating membrane functions of some proteins (Edidin, 1974). In order to obtain a molecular level understanding of the structure and dynamics of biomembranes, the lateral diffusion of phospholipids and proteins in biomembranes (Cherry, 1979; Hackenbrock, 1981; Peters, 1981) and multilayers of phospholipid bilayers (Devaux and McConnell, 1972; Scandella et al., 1972; Trauble and Sackmann, 1972; Galla and Sackmann, 1974a, b; Vanderkooi et al., 1975; Wu et al., 1977; Smith and McConnell, 1978; Kano et al., 1981; Smith et al., 1981; Miller and Evans, 1989; Almeida et al., 1992) has been extensively studied.

In recent years, monolayers at the air-water interface have received much attention as model membrane systems (Stroeve and Miller, 1975; Teissie et al., 1978; Loughran et al., 1980; Peters and Beck, 1983; Subramanian and Patterson, 1985; Bohorquez and Patterson, 1988; Meller et al., 1989; Caruso et al., 1991; Kim and Yu, 1992; Caruso et al., 1993a). Air-water monolayers of amphiphilic lipids resemble half a biological membrane and thus can serve as an excellent model for biomembranes. The air-water monolayer is a particularly useful model system in which to study the lateral diffusion of amphiphiles because it facilitates the study of a number of parameters, including the nature and packing characteristics of the lipid molecules, as well as the temperature and the nature of the subphase. In addition, lipid monolayers at the air-water interface can act as a model system in which to study the basic characteristics of low-dimensionality systems.

Several experimental techniques have been applied in studies of lateral diffusion of lipids at air-water monolayers. Values of the lateral diffusion coefficients have been most commonly determined from fluorescence recovery after photobleaching (FRAP) experiments (Teissie et al., 1978; Peters and Beck, 1983; Meller et al., 1989; Kim and Yu, 1992) or from the analysis of the kinetics of pyrene excimer formation (Loughran et al., 1980; Subramanian and Patterson, 1985; Bohorquez and Patterson, 1988). The disadvantages and complications associated with obtaining lateral diffusion coefficients using these techniques have been reported previously (Axelrod, 1977; Peters and Beck, 1983; Caruso et al., 1991).

We have recently reported mutual lateral diffusion coefficients for amphiphiles in monolayers at the air-water interface, determined from fluorescence quenching data (Caruso et al., 1991, 1993b). As an extension to these studies, the present study deals with the fluorescence quenching of a pyrene-labeled phospholipid embedded in two phospholipid matrices, by two amphiphilic quenchers, and focuses on developing a better understanding of diffusion of amphiphiles in air-water monolayers.

Received for publication 23 April 1993 and in final form 9 September 1993.
Address reprint requests to Dr. Franz Grieser.

0006-3495/93/12/2493/11 $2.00

MATERIALS AND METHODS

Materials

N-(1-pyrenesulfonyl)dipalmitoyl-L-α-phosphatidylethanolamine (pyrene-DPPE) and 4-(*N,N*-dimethyl-*N*-hexadecyl)ammonium-2,2,6,6-tetrameth-

ylpiperidine-1-oxyl, iodide (CAT-16) were purchased from Molecular Probes, Inc. Dipalmitoyl-L-α-phosphatidylcholine (DPPC) and dimyristoyl-L-α-phosphatidylcholine (DMPC) were obtained from Sigma Chemical Co. *N,N*-octadecyldimethylamine (ODDMA) was from Pfaltz and Bauer, Inc., and sodium perchlorate (analytical reagent (AR) grade) was from Merck. Sodium hydroxide (AR grade) was purchased from Ajax Chemicals. All chemicals were used without further purification. All nonaqueous solvents were spectroscopic grade and were obtained from Ajax Chemicals or Merck. "Milli-Q" water was used to prepare the subphase (conductivity $< 1 \times 10^{-6}$ S cm^{-1}, surface tension = 72 mN m^{-1} at 25°C). Chloroform was used as the spreading solution for all monolayer experiments.

Surface pressure-area measurements

Surface pressure-area (π-A) measurements of the pure amphiphile monolayers were conducted on a 57.9 × 13.5 cm^2 poly(tetrafluoroethylene) (PTFE) Langmuir trough, with a PTFE barrier, driven at a compression rate of 0.03 nm^2 $molecule^{-1}$ min^{-1}. A 59.7 cm × 16.5 cm^2 PTFE Langmuir trough with a compression rate of 0.05 nm^2 $molecule^{-1}$ min^{-1} and a 47.0 × 15.0 cm^2 PTFE Langmuir trough (KSV-2200) (compression rate 0.05 nm^2 $molecule^{-1}$ min^{-1}) equipped with a quartz window in the bottom were used for steady-state monolayer fluorescence experiments. The KSV-2200 trough was also used for time-resolved monolayer fluorescence experiments.

All surface pressure-area measurements were made by the Wilhelmy hanging plate method (Heimenz, 1977). For π-A measurements of the pure amphiphiles and steady-state monolayer fluorescence measurements, a 4.3-cm mica plate suspended from a Shinkoh 2-g capacity strain gauge was used. The apparent changes in weight with monolayer compression were converted to voltages by the strain gauge and recorded on an Apple Macintosh PC. A 3.0-cm roughened platinum plate suspended from a Cahn microbalance was used in the time-resolved monolayer fluorescence measurements. The change in voltage from the microbalance was monitored by a KSV-2200 trough controller and recorded on an IBM PC with software from KSV (Helsinki).

Experiments were initiated by filling the trough with the appropriate subphase. Approximately 10^{17} molecules from 1 mM chloroform solutions mixed to the desired ratio were spread onto the subphase, using a 100-μl SGE syringe. The solvent was then allowed to evaporate for 10 min, after which the monolayer was compressed as desired.

Steady-state monolayer fluorescence measurements

Steady-state fluorescence measurements were performed on two different experimental set-ups. The first set-up, located at the University of Melbourne, employed a Perkin-Elmer LS-5 luminescence spectrophotometer; details of the complete system have been given previously (Caruso et al., 1991). Briefly, two silica fibre optic bundles were used to transfer the exciting light and the fluorescence to and from the monolayer. Since the fluorescence signal from the monolayer was small, it was necessary to subtract the background signal due to scatter from the subphase of the exciting light and/or fluorescence from the PTFE. The background signal, monitored at the same emission wavelength as that of pyrene-DPPE, was recorded for 10 min, averaged, and then subtracted from the fluorescence signal when the monolayer was present. Fluorescence intensity curves as a function of monolayer compression were obtained using this experimental set-up (Figs. 2 and 4). Thus the fluorescence intensities at various surface pressures (I values) were obtained for each of the monolayers of different quencher concentration. The I_o value at a given surface pressure was obtained from a monolayer containing only pyrene-DPPE in the lipid matrices DMPC or DPPC (reference monolayers). Addition of the quencher CAT-16 to the monolayer films of DMPC and DPPC did not significantly affect the packing of the molecules, and in all cases the isotherms were within ±0.02 nm^2 $molecule^{-1}$ of each other both in the absence and presence of CAT-16. The addition of ODDMA quencher to the monolayer film of DMPC, however, caused a reduction in area, at a particular surface pressure, with the isotherms differing in average area per molecule by ~0.07 nm^2 at the high end of the concentration range of ODDMA (25 mole %). This resulted in a different surface concentration of pyrene-DPPE molecules for the reference monolayer and for monolayers containing quencher. To account for this variation in average area per molecule, and for the dependence of the fluorescence lifetime of pyrene-DPPE on the average area per molecule, it was necessary to apply a correction for the pyrene-DPPE/ODDMA/DMPC system in the following manner. All fluorescence intensities were scaled to constant surface concentration of pyrene-DPPE and then further corrected for the variation of fluorescence lifetime of pyrene-DPPE with average area per molecule (see later).

In the second set-up (University of Uppsala), a silica lens and mirrors were used to focus the excitation light from a pulsed (20 Hz) nitrogen laser (λ_{em} = 337 nm) (WSL-337ND; Laser Science, Inc., Cambridge, MA) onto the monolayer. The exciting light was then passed through a quartz window in the bottom of the trough and into a black box, which acted as a light sink, reducing the intensity of the scattered light. The emission was collected and transmitted to an optical multichannel analyzer (EE&G model 1460) by means of a silica optical fiber positioned at a right angle to the surface. The typical exposure time was 20 s. Details are described elsewhere (Wistus et al., 1992). Spectra obtained using this experimental set-up are shown in Figs. 3 and 5.

Time-resolved monolayer fluorescence measurements

Fluorescence decay curves were measured by the time-correlated single-photon counting method (O'Connor and Phillips, 1984). The decay measurements were made at the University of Uppsala using frequency-doubled (320 nm) radiation from a 4-dicyanomethylene-2-methyl-6-*p*-dimethylaminostyryl-4H-pyran dye laser (Spectra Physics model SP 375 and 344S) synchronously pumped by a mode-locked, Nd:YAG laser (Spectra Physics model SP 3800). The exciting light was focused onto the monolayer by means of a lens and mirrors and passed through a quartz window in the bottom of the trough. The emission from the monolayer was focused by a fused silica lens onto a Hamamatsu (model R15640) microchannel plate photomultiplier tube, having passed through a polarizer set so as to remove distortion of decay curves by rotational relaxation. The wavelength of observation (400 nm) was determined by an Oriel narrow-band pass filter and an Oriel low-fluorescence cut-off filter. The electronics and analysis software have been described elsewhere (Wistus et al., 1992).

The time-resolved fluorescence measurements showed a weak fast decay component attributable to fluorescence from the PTFE trough. This background decay was subtracted from the measured decays to yield the true decay curves. A photodiode (model BPW 34; Elfa, Ltd.) connected to a voltage/frequency converter and counter monitored the exciting light and gated the detection system to ensure the background and monolayer decays were recorded with the same overall excitation intensity. The typical exposure time was 20 min.

As mentioned earlier, the average area per pyrene-DPPE molecule at a given surface pressure differs for the monolayers with and without ODDMA quencher. As the fluorescence lifetime of pyrene-DPPE was found to vary with average area per molecule, the unquenched lifetime needed for the analysis of any particular experiment was first corrected to the value appropriate for the average area per molecule involved.

THEORY

The fluorescence decay following a delta pulse excitation for a two-dimensional system is given by the expression (Medhage and Almgren, 1992; Medhage, 1993)

$$\ln \frac{F(t)}{F(0)} = -k_o t - \tfrac{1}{2} a^2 c_o Q_2(ha, t/\tau_q) \qquad (1)$$

with Q_2 (ha, t/τ_q) equal to

$$\frac{16}{\pi}\int_0^\infty \frac{1-\exp[-(t/\tau_q)x^2}{[xJ_1(x)+haJ_0(x)]^2+[xY_1(x)+haY_0(x)]^2}\,\frac{dx}{x^3} \quad (2)$$

where k_o is the natural decay constant, which is determined in a separate experiment; a is the probe-quencher encounter distance; c_o is the quencher concentration (molecules/Å^2), $h = k_q a/2D$ and is thus a parameter that weights reaction against diffusion; where k_q is the first-order quenching rate constant for the P^*-Q pair, D is the mutual diffusion coefficient of the probe and quencher ($D = D_P + D_Q$), and $\tau_q = a^2/D$. $J_n(x)$ and $Y_n(x)$ are the Bessel functions of the first and second kind, respectively, of order n.

The integral expression in Q_2 is difficult to handle numerically, and therefore two-dimensional diffusion has been analyzed in detail only for the diffusion-controlled case, in which Eq. 2 simplifies to that given by Owen (1975),

$$Q_{2,\infty} = Q_2(ha=\infty, t/\tau_q) = \frac{16}{\pi}\int_0^\infty \frac{1-\exp[-(t/\tau_q)x^2]}{J_0^2(x)+Y_0^2(x)}\,\frac{dx}{x^3}. \quad (3)$$

Owen presented the following approximation to this integral in the range $0 \le t \le 10\tau_q$:

$$Q_{2,\infty} = 14.180\sqrt{t/\tau_q} + 3.17t/\tau_q. \quad (4)$$

This approximation, however, underestimates the value of $Q_{2,\infty}$ by more than 10% when $t/\tau_q \ge 1$.

Medhage and Almgren (1992) have created an approximation to Eq. 2 by calculating Q_2 for a large set of ha and t/τ_q values and by describing the dependence of Q_2 on ha and t/τ_q by the function

$$Q_2^*(ha, t/\tau_q) = \frac{[A_1(t/\tau_q)^\alpha + A_2\sqrt{t/\tau_q}]ha}{A_3(t/\tau_q)^\beta + A_4/\sqrt{t/\tau_q} + ha} \quad (5)$$

where α, β, and A_1–A_4 are parameters determined for different ranges of t/τ_q values.

The fluorescence decay data were nonlinear least squares (NLLS) fitted to Eq. 1 with the approximation Q_2^* using a modified Levenberg-Marquardt algorithm (Bevington, 1969), which eliminates the need for partial derivatives. The reduced χ^2 value was used to judge the quality of the fit. In the analysis for the determination of the lateral diffusion coefficients, the lifetime value of pyrene-DPPE in the monolayer at a particular surface pressure was used (measured in a separate experiment) with values of 1.0 and 0.8 nm for the encounter distances for pyrene-DPPE quenched by CAT-16 and pyrene-DPPE quenched by ODDMA, respectively. The encounter distances were calculated as the sum of the molecular radii, which in turn were calculated from the limiting molecular areas obtained from the surface pressure-area isotherms. The expanded nature of the CAT-16, ODDMA, and pyrene-DPPE monolayers introduces some uncertainty into the determination of the interaction distances (Caruso et al., 1991).

The relation between the steady-state fluorescence intensity and quencher concentration for diffusion-controlled quenching in two dimensions has the same functional form as the expression in three dimensions (Owen, 1975) and is given by

$$\frac{I_o}{I} = \frac{x\tau_f}{[1 - y(\pi/x)^{1/2}\exp(y^2/x)\mathrm{erfc}(y/(x)^{1/2})]} \quad (6)$$

where $x = 1/\tau_f + 2.28[Q]D$ and $y = 3.72D^{1/2}a[Q]$. I_o and I refer to the steady-state fluorescence intensity in the absence and presence, respectively, of quencher molecules, $[Q]$ is the quencher concentration (molecules/Å^2), D is the mutual diffusion coefficient of the probe and quencher ($D = D_P + D_Q$), a is the probe-quencher encounter distance, and τ_f is the fluorescence lifetime in the absence of quencher molecules. The function erfc(x) is the complementary error function as defined in standard mathematical tables. The numerical values in the above equation have been calculated for the time range of $t/\tau_q \le 5$ (Caruso et al., 1991, 1993b) and differ slightly from those reported by Owen (1975). This time range has been used by taking into account the approximate lifetime of pyrene-DPPE in the air-water monolayers.

The steady-state fluorescence quenching data were NLLS fitted to Eq. 6 with lifetime values of pyrene-DPPE, at a given surface pressure, in the monolayer, and a value of 1.0 nm for the encounter distance for pyrene-DPPE with CAT-16, and 0.8 nm for pyrene-DPPE with ODDMA.

RESULTS

Surface pressure-area isotherms

The surface pressure-area (π-A) isotherms of the pure amphiphiles were measured in order to investigate the monolayer behavior and stability of the components at the air-water interface. The isotherms have also been used to calculate the encounter distances required for determination of the lateral diffusion coefficients.

The surface pressure-area (π-A) isotherms of the pure amphiphiles, obtained by continuous compression, are shown in Fig. 1. The π-A isotherm of DPPC shows a plateau region, which is interpreted as a transition between the liquid-expanded (LE) and the liquid-condensed (LC) phase (Peters and Beck, 1983; Tamm and McConnell, 1985). In contrast, CAT-16, DMPC, and pyrene-DPPE produce isotherms that have no inflections or plateau regions, which suggests that there are no phase transitions in these monolayers. They exhibit a LE phase at all measured surface pressures. These π-A isotherms are in good agreement with those reported previously (Tamm and McConnell, 1985; Caruso et al., 1991, 1993a). The π-A isotherms of DMPC and pyrene-DPPE measured on a 0.1 M $NaClO_4$ subphase were found to be identical to those measured on a basic 0.1 M $NaClO_4$ subphase. Stability of ODDMA at the air-water interface was

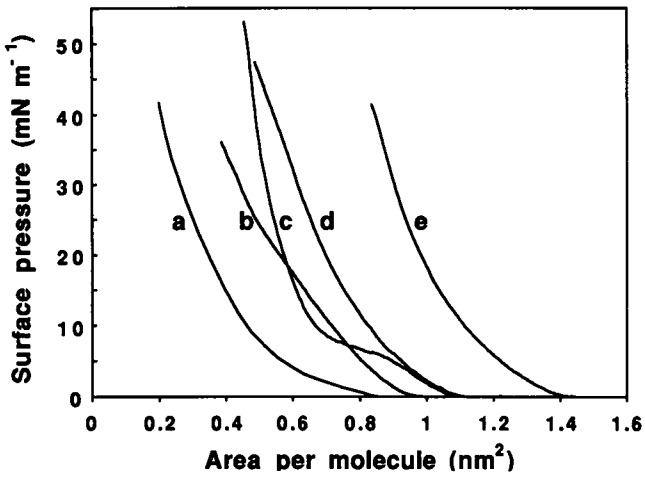

FIGURE 1 Surface pressure-area isotherms of the pure amphiphile monolayers on a 0.1 M $NaClO_4$ subphase at 20 ± 1°C: (*a*) ODDMA; (*b*) CAT-16; (*c*) DPPC; (*d*) DMPC; (*e*) pyrene-DPPE.

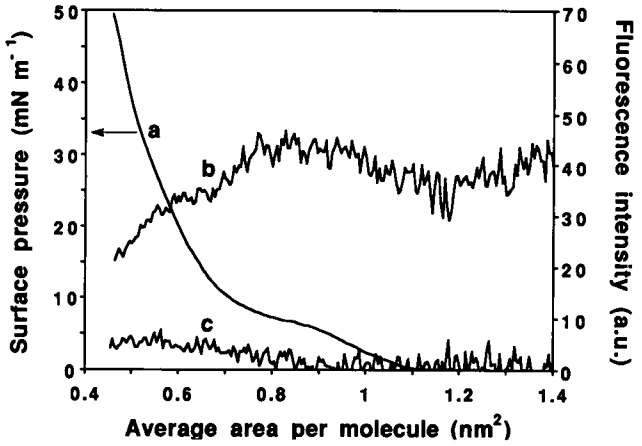

FIGURE 2 Normalized steady-state fluorescence behavior of 2 mole % pyrene-DPPE in a DPPC monolayer during monolayer compression. (*a*) surface pressure-area isotherm of 2 mole % pyrene-DPPE diluted into DPPC; *b* and *c* are the normalized fluorescence intensity versus area per molecule curves for monomer and excimer emission; (*b*) monomer, λ_{em} = 400 nm; (*c*) excimer, λ_{em} = 500 nm. Excitation wavelength = 350 nm. Temperature = 20 ± 1°C. Subphase: 0.1 M $NaClO_4$.

only obtained by incorporating 0.1 M $NaClO_4$ in the subphase. The pH was adjusted to 12.5 to prevent protonation of the amino group and consequent loss of quenching capacity. The π-A isotherm is of the LE type, with no discontinuities suggestive of phase changes.

Surface pressure isotherms of the mixed monolayers containing probe, quencher, and diluent (in mole percentages used in the quenching experiments) were recorded to determine whether the presence of the probe and quencher molecules in the film affected the packing properties of the pure diluent. The π-A isotherms recorded for the mixed monolayers of pyrene-DPPE and CAT-16 or ODDMA diluted with DMPC showed the monolayer to be in the LE state at all measured surface pressures. The isotherms of the mixed monolayers containing CAT-16 showed little deviation from the isotherm of pure DMPC. Addition of ODDMA to the monolayer film caused a significant decrease in the average area per molecule of the isotherm of pure DMPC (see above). The isotherms of the mixed monolayers of pyrene-DPPE, CAT-16, and DPPC were similar to that of pure DPPC.

Steady-state fluorescence

Fig. 2 shows the normalized steady-state monomer (400 nm) and excimer (500 nm) emission intensities monitored as a function of monolayer compression for a 2 mole % pyrene-DPPE/DPPC monolayer. Above an average area of 1.10 nm^2 molecule^{-1}, there is an equilibrium between gaseous and LE phases that results in heterogeneous lipid distribution (Lösche et al., 1983). If the fluorescence intensity is monitored over time, fluctuations in the fluorescence intensity are observed, which is indicative of large mobile domains. In this region there is no correlation between fluorescence intensity and surface concentration of pyrene-DPPE.

Fig. 2 shows no large domains were detected by continuous compression of the monolayer. At average areas per molecule between about 0.85 and 1.10 nm^2, the monolayer is in the LE state, where we have a homogeneous fluid monolayer with a decreasing compressibility as the monolayer is compressed (Tamm and McConnell, 1985). Pyrene-DPPE has a LE-type isotherm and is therefore expected to be miscible in the LE phase of the DPPC monolayer (Dörfler, 1990; Urquhart et al., 1992). Fig. 2 shows only monomer emission in this region, which indicates that the two components are miscible in the monolayer film. This is in agreement with the work of Dörfler (1990), who reported that if two phospholipids individually exhibit LE behavior, they are miscible in any proportion, independent of the chemical structure of the components.

Further compression of the monolayer results in a plateau region that has been reported to be a coexistence region of LE and LC phases where LC domains form periodic patterns (Peters and Beck, 1983; Tamm and McConnell, 1985). Fig. 2 shows that at the onset of this region (~0.85 nm^2 molecule^{-1}) there is a gradual increase in the excimer intensity and a corresponding decrease in the monomer emission. The presence of excimer emission provides evidence that pyrene-DPPE is phase separated and/or aggregated in this region.

At an average area per molecule of about 0.65 nm^2, the LC lipid domains are interconnected but still coexist with fluid lipid, and at areas below 0.55 nm^2 molecule^{-1} all lipid is in a solid state (Tamm and McConnell, 1985). The probe molecules are immiscible in these regions of the isotherm. Similar mixing behavior for dye molecules in DPPC monolayers at the air-water interface has been reported in the literature (Peters and Beck, 1983; Meller, 1988; Urquhart et al., 1992).

The fluorescence spectra (excitation 337 nm) for a 2 mole % pyrene-DPPE/DPPC monolayer recorded at various areas per molecule are shown in Fig. 3. The fluorescence spectrum at an average area per molecule of 1.05 nm^2 (LE phase) shows peaks at 378, 397, and 417 (shoulder) nm, with only monomer emission observed. Further compression to 0.95

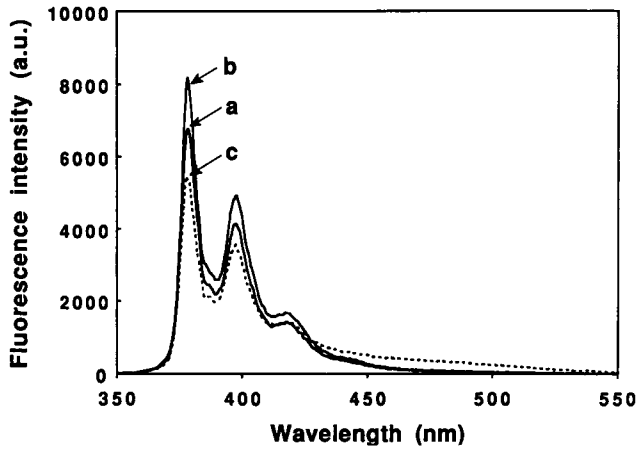

FIGURE 3 Steady-state fluorescence spectra of a 2 mole % pyrene-DPPE/DPPC monolayer at different average areas per molecule. (*a*) 1.05 nm^2; (*b*) 0.95 nm^2; (*c*) 0.48 nm^2. Excitation wavelength = 337 nm. All spectra were recorded at 20 ± 1°C. Subphase: 0.1 M $NaClO_4$.

nm^2 $molecule^{-1}$ (LE phase) results in no change in the structure of the fluorescence spectrum but shows an increase in fluorescence intensity. The increase in fluorescence intensity can be attributed to an increase in concentration and an increase in lifetime upon monolayer compression (Caruso et al., 1993a). The fluorescence spectrum in the solid phase at an average area per molecule of 0.48 nm^2 shows a "tail" around 480 nm, which is characteristic of the formation of excimers of pyrene (Espenson, 1981). This indicates that pyrene-DPPE is aggregated in the monolayer film, and as a consequence, the monomer intensity is reduced as a result of excimer formation and/or concentration quenching.

Curve *a* in Fig. 4 shows the steady-state fluorescence intensity monitored as a function of monolayer compression for *a* of 2 mole % pyrene-DPPE/DMPC monolayer. Only monomer emission is seen. The fluorescence spectra (excitation 337 nm) for this monolayer at various surface pressures are shown in Fig. 5. Only the characteristic monomer peaks are observed, which indicates that pyrene-DPPE is not aggregated in the monolayer film. The nonlinear increase in fluorescence intensity with surface concentration of pyrene-DPPE (as a result of compression of the monolayer) has recently been attributed to diminished oxygen quenching with increasing surface pressure (Caruso et al., 1993a).

The fluorescence emission spectra of the mixed monolayers containing pyrene-DPPE and CAT-16 or ODDMA diluted with either DPPC (only in the LE phase) or DMPC showed monomer emission only. The fluorescence intensities from these monolayers were also constant with time. Both of these observations indicate homogeneous mixing of the monolayer components (Caruso et al., 1991; Urquhart et al., 1992; Caruso et al., 1993a).

For the analysis of diffusional quenching data and hence, determination of lateral diffusion coefficients from a two-dimensional environment, a single exponential decay time for the fluorophore in the absence of quencher is required. Thus, steady-state and time-resolved quenching measurements for the DPPC matrix were performed only in the LE phase of the surface pressure-area isotherm.

Steady-state quenching measurements

We have previously shown that pyrene-DPPE is quenched by CAT-16 at a diffusion controlled rate both in homogeneous solution and in different matrix air-water monolayers (Caruso et al., 1993a, b). Quenching of pyrene-DPPE by ODDMA in methanol solution is somewhat slower ($k_q = 8.5 \times 10^8$ M^{-1} s^{-1}) than the diffusion limited rate ($k_q = 6 \times 10^9$ M^{-1} s^{-1}) estimated from the Debye-Smoluchowski equation for a diffusion-controlled reaction in solution (Espenson,

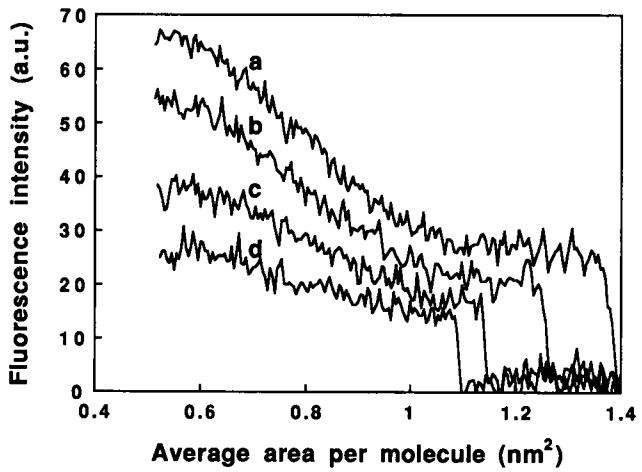

FIGURE 4 Steady-state monomer fluorescence intensity of a 2 mole % pyrene-DPPE/DMPC monolayer as a function of monolayer compression for different amounts of CAT-16. (*a*) 0 mole %; (*b*) 5 mole %; (*c*) 10 mole %; (*d*) 15 mole %. λ_{ex} = 350 nm and λ_{em} = 400 nm. Temperature = 20 ± 1°C. Subphase: 0.1 M $NaClO_4$.

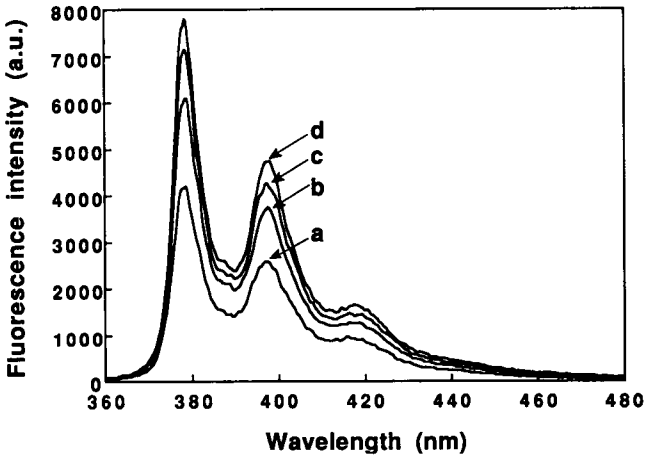

FIGURE 5 Steady-state fluorescence spectra of a 2 mole % pyrene-DPPE/DMPC monolayer at different surface pressures. (*a*) π = 5 mN m^{-1}, average area = 0.92 nm^2 $molecule^{-1}$; (*b*) π = 15 mN m^{-1}, average area = 0.76 nm^2 $molecule^{-1}$; (*c*) π = 25 mN m^{-1}, average area = 0.66 nm^2 $molecule^{-1}$; (*d*) 35 mN m^{-1}, average area = 0.57 nm^2 $molecule^{-1}$. Excitation wavelength = 337 nm. All spectra were recorded at 20 ± 1°C. Subphase: 0.1 M $NaClO_4$.

1981). This indicates that there is a small activation energy barrier to quenching and may lead to underestimated lateral diffusion coefficients. The quenching efficiency of aromatics by amines is known to be polarity sensitive (Birks, 1970), and if the effective polarity at the air-water interface is greater than that of methanol, the quenching of pyrene-DPPE by ODDMA may proceed at a faster rate. Furthermore, ODDMA has been shown to efficiently quench pyrene-DPPE in dioleoyl-L-α-phosphatidylcholine (DOPC) monolayers (Caruso et al., 1993a) and therefore has been employed in this study.

Fig. 4 shows the steady-state fluorescence intensity (monitored at 400 nm) for a 2 mole % pyrene-DPPE/DMPC monolayer as a function of monolayer compression for different concentrations of CAT-16 quencher. Curve *a* is the unquenched fluorescence intensity, and curves *b*, *c*, and *d* are the quenched curves containing 5, 10, and 15 mole % of CAT-16, respectively. Fig. 4 clearly shows that CAT-16 efficiently quenches the fluorescence of pyrene-DPPE embedded in a DMPC monolayer, with the degree of quenching increasing as the concentration of CAT-16 is increased. The quenching curves as a function of compression for pyrene-DPPE quenched by ODDMA in a DMPC monolayer, and for pyrene-DPPE quenched by CAT-16 in a DPPC monolayer (LE phase), show similar quenching behavior (data not shown).

The ratio of the fluorescence intensity in the absence of quencher to the quenched fluorescence intensity, at a given surface pressure, can be calculated from Fig. 4. Stern-Volmer plots for the quenching of 2 mole % pyrene-DPPE by CAT-16 in a DMPC and a DPPC monolayer, at various surface pressures, are shown in Fig. 6. Fig. 7 shows the corresponding plot for the quenching of pyrene-DPPE by

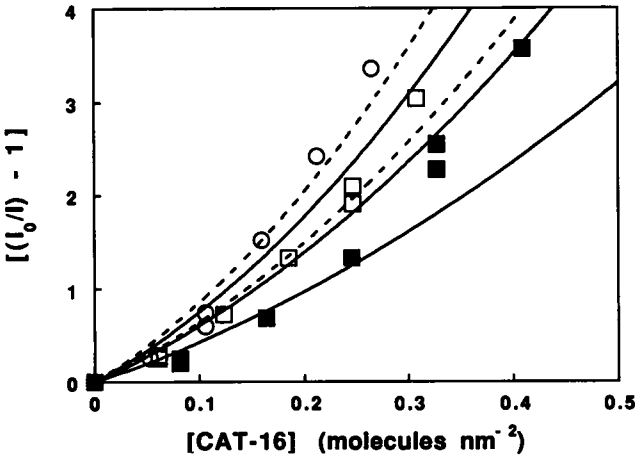

FIGURE 6 Stern-Volmer plots for the quenching of 2 mole % pyrene-DPPE by CAT-16 in DPPC and DMPC monolayers at various surface pressures. ○, DPPC, 3 mN m^{-1}; □, DMPC, 10 mN m^{-1}; ■, DMPC, 30 mN m^{-1}. λ_{ex} = 350 nm and λ_{em} = 400 nm. Temperature = 20 ± 1°C. Subphase: 0.1 M $NaClO_4$. The solid curves are the theoretical fits to the experimental data calculated using Eq. 6, with parameters given in the text. The dashed curves represent theoretical fits for a variation of ±20% in the diffusion coefficient for the DPPC data.

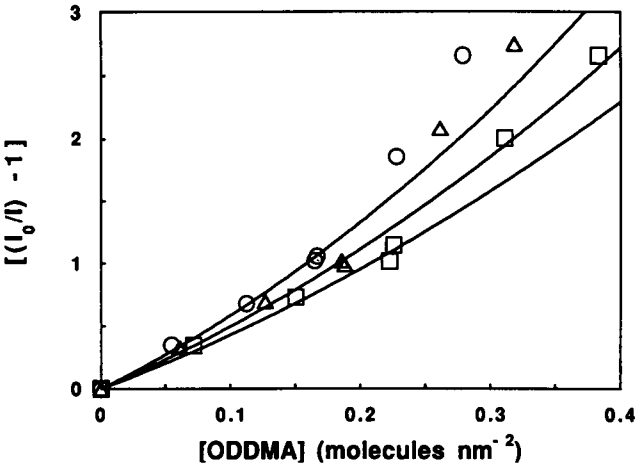

FIGURE 7 Stern-Volmer plots for the quenching of 2 mole % pyrene-DPPE by ODDMA in DMPC monolayers at various surface pressures. ○, 5 mN m^{-1}; △, 10 mN m^{-1}; □, 20 mN m^{-1}. λ_{ex} = 350 nm and λ_{em} = 400 nm. Temperature = 20 ± 1°C. Subphase: 0.1 M $NaClO_4$. The solid curves are the theoretical fits to the experimental data calculated using Eq. 6, with parameters given in the text.

ODDMA in a DMPC monolayer at various surface pressures. The quenching behavior in each of the systems studied shows the expected upward curvature characteristic of quenching in a two-dimensional environment (Owen, 1975; Kano et al., 1981; Caruso et al., 1991, 1993b). Eq. 6 was used to calculate the lateral diffusion coefficients from the steady-state quenching data. The solid curves in Figs. 6 and 7 are the NLLS best-fit curves to the experimental steady-state quenching data for 5, 10, and 15 mole % quencher. The 20 and 25 mole % data have been omitted from the fits (see later). An indication of the magnitude of the error in the diffusion coefficient is given by the dashed curves in Fig. 6, which represent theoretical fits for a variation of ±20% in the diffusion coefficient for the DPPC data. The values of the lateral diffusion coefficients are given in Table 1.

Time-resolved quenching measurements

Time-resolved fluorescence spectroscopy allows the detection of aggregated species, which have lifetimes different from those of the monomeric species and do not contribute significantly to the intensity of the steady-state spectra. Thus, the emission of the aggregated species may not be clearly observed in the fluorescence spectrum (possibly due to a low quantum yield of fluorescence) but will result in nonexponential decay behavior of the temporal response of the emission. Moreover, the comparison of time-resolved and steady-state results can demonstrate the presence of static quenching (Weber, 1966). Time-resolved measurements were therefore performed on the monolayer systems covered by the steady-state experiments over the same surface pressure range.

Fig. 8 shows the fluorescence decay behavior of a 2 mole % pyrene-DPPE/DMPC monolayer at surface pressures of 5, 15, and 25 mN m^{-1}. The decays are best fitted by a single-exponential function, indicating that pyrene-DPPE is not ag-

TABLE 1 Fluorescence decay lifetimes and mutual lateral diffusion coefficients for 2 mole % pyrene-DPPE diluted with DPPC or DMPC measured for different surface pressures on 0.1 M $NaClO_4$

			$D \times 10^7/cm^2\ s^{-1}$				
			Steady state		Time-resolved		
Matrix	π/mN m^{-1}	τ_o/ns	CAT-16	ODDMA	CAT-16 (10%)	CAT-16 (20%)	ODDMA* (20%)
DPPC	3	7.2	7.9	—	1.7	1.4	—
DMPC	5	6.4	5.7	8.3	1.3	2.2	0.65
	10	7.6‡	5.4	5.5	—	—	—
	15	8.8	4.5	4.0	0.69	0.91	0.44
	20	9.9‡	3.1	3.4			
	25	11.2	2.5	2.9	0.50	0.38	0.27
	30	12.3	2.0	2.6	0.32	0.32	0.20
	35	13.2	1.7	2.3	0.22	0.23	0.16

Excitation wavelength = 320 nm, emission wavelength = 400 nm, temperature = 20 ± 1°C.

* The fluorescence lifetimes used in determining these values have been corrected for differences in the average areas per molecule between the reference monolayer and monolayers containing ODDMA quencher (see text). The lifetime values for 5, 15, 25, 30, and 35 mN m^{-1} are 6.9, 10.4, 13.6, 15.0, and 16.3 ns, respectively.

‡ These lifetime values have been calculated from a linear fit to the experimental data since there is a linear relationship between the lifetime of pyrene-DPPE and surface pressure in the DMPC matrix (Caruso et al., 1993a).

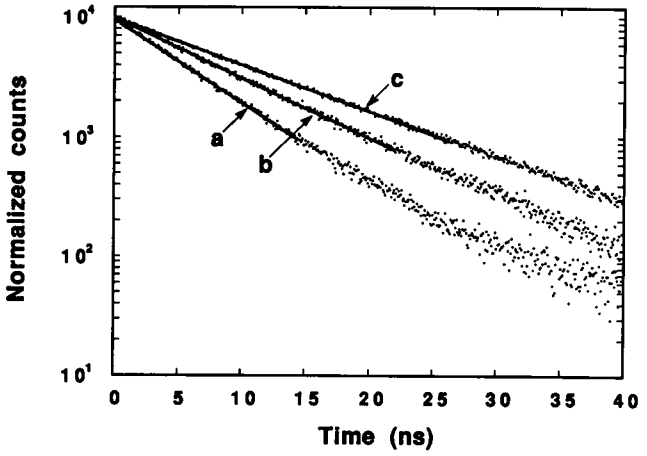

FIGURE 8 Fluorescence decays of a 2 mole % pyrene-DPPE/DMPC monolayer at various surface pressures. (*a*) π = 5 mN m^{-1}; (*b*) π = 15 mN m^{-1}; (*c*) π = 25 mN m^{-1}. Subphase: 0.1 M $NaClO_4$. λ_{ex} = 320 nm and λ_{em} = 400 nm. Temperature = 20 ± 1°C. All fluorescence decays have been normalized to the same maximum intensity.

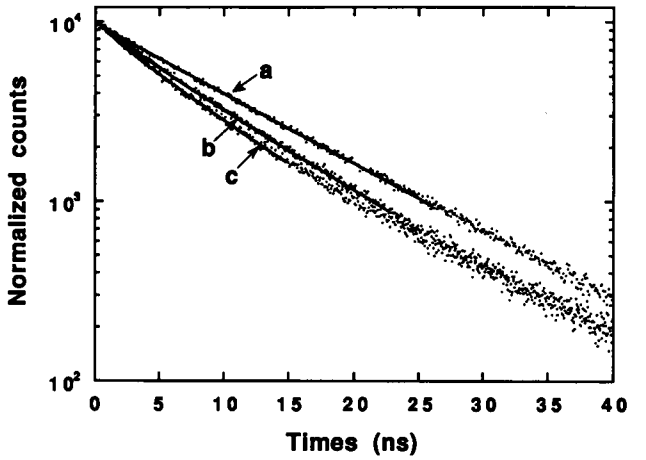

FIGURE 9 Fluorescence decays of a 2 mole % pyrene-DPPE/DMPC monolayer for various concentrations of CAT-16 at π = 25 mN m^{-1}. (*a*) 0 mole % CAT-16; (*b*) 10 mole % CAT-16; (*c*) 20 mole % CAT-16. All fluorescence decays have been normalized to the same maximum intensity. Subphase: 0.1 M $NaClO_4$. λ_{ex} = 320 nm and λ_{em} = 400 nm. Temperature = 20 ± 1°C.

gregated in the monolayer film. The values of the fluorescence lifetimes at different surface pressures are given in Table 1. The fluorescence decay curves at 25 mN m^{-1} for this monolayer, quenched by CAT-16, are shown in Fig. 9. The quenched decays (curves *b* and *c*) are clearly nonexponential, as expected for diffusional quenching in a two-dimensional environment (Owen, 1975; Medhage and Almgren, 1992). The solid lines are the fitted curves, and the results of the fittings are shown in Table 1. The fluorescence decays observed for the quenching of pyrene-DPPE by ODDMA in a DMPC monolayer are also nonexponential (data not shown) and are well described by the theory of diffusional quenching in two dimensions.

The fluorescence decays for 2 mole % pyrene-DPPE diluted with DPPC, at different areas per molecule, are shown in Fig. 10. The fluorescence decay curve *a* was recorded at an average area per molecule of 0.97 nm^2 and follows single-exponential decay kinetics, which confirms that pyrene-DPPE is miscible in the LE phase of DPPC. The solid line is a fit to a single exponential decay function and yields a value of 7.2 ns for the decay time. The decay behavior of this monolayer becomes nonexponential at higher compression, as shown by the fluorescence decay curves *b* and *c*. The fluorescence decay curve *b* was measured at an average area per molecule of 0.69 nm^2 and the fluorescence decay curve *c* at 0.49 nm^2. This nonexponentiality shows that pyrene-DPPE is aggregated when the monolayer film is in a phase other than the LE phase of DPPC. These results are in agreement with the steady-state measurements. The solid lines in

Fig. 10 represent fits to a double-exponential decay function. Fig. 11 shows the quenching of 2 mole % pyrene-DPPE by 10 mole % CAT-16 (curve *b*) and 20 mole % (curve *c*) CAT-16 in DPPC at an average area of 0.97 nm^2 $molecule^{-1}$ (LE phase). The solid curves are NLLS fits to the experimental data, obtained from Eq. 1 with the approximation Q_2*. The lateral diffusion coefficients obtained are given in Table 1.

DISCUSSION

Table 1 clearly shows that the lateral diffusion coefficient for the matrix monolayer DMPC, using either CAT-16 or ODDMA as quencher, decreases as the surface pressure increases. A decrease in the lateral diffusion coefficient with surface pressure is observed for both steady-state and time-resolved fluorescence measurements. This observation reflects the expected decrease of monolayer fluidity with compression (Peters and Beck, 1983; Caruso et al., 1991, 1993b).

Examination of Table 1 shows that the lateral diffusion coefficients obtained from steady-state measurements are significantly larger than those obtained from time-resolved data. For the steady-state measurements, the quencher concentration ranges from a value of 5 to 25 mole %. The 20 and 25 mole % experimental data points for the quenching of pyrene-DPPE by CAT-16 in DMPC or DPPC monolayers, as shown in Fig. 6, clearly show positive deviation from the theoretical curves that fit the lower quencher concentration data. This is also observed in Fig. 7 for ODDMA as the quencher molecule. This positive deviation of the experimental data points from the calculated curves is characteristic of static quenching (Weber, 1966). Since static quenching would be more pronounced at higher concentration levels, the 20 and 25 mole % experimental data points have been omitted from the fits (Figs. 6 and 7). The fact that the steady-state data give higher diffusion coefficients for both the DMPC and DPPC systems than do the time-resolved data also suggests that static quenching is influencing the emission intensity in the steady-state measurements. The model used for analysis of the steady-state data does not take into account static quenching, and therefore reliable lateral diffusion coefficients are not obtainable from the data. Further evidence for static quenching comes from the difference between the calculated lateral diffusion coefficients obtained from the steady-state and time-resolved data being greatest at high surface pressure (with the exception for the pyrene-DPPE/ODDMA/DMPC system at 5 mN m^{-1}), where diffusion is minimal and hence any contribution from static quenching would be most evident.

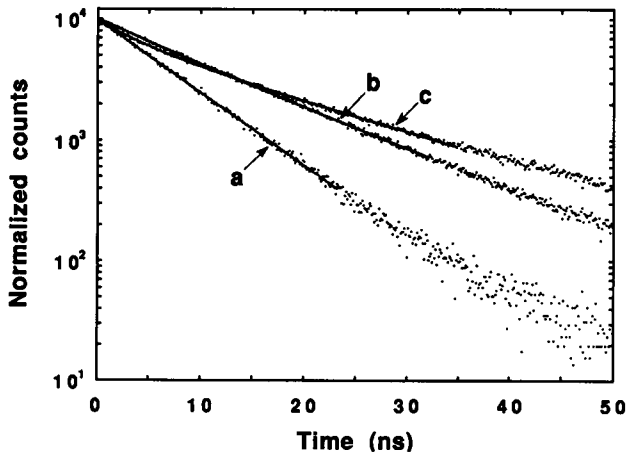

FIGURE 10 Fluorescence decays of a 2 mole % pyrene-DPPE/DPPC monolayer at different average areas per molecule. (*a*) 0.97 nm^2; (*b*) 0.69 nm^2; (*c*) 0.49 nm^2. Subphase: 0.1 M $NaClO_4$. λ_{ex} = 320 nm and λ_{em} = 400 nm. Temperature = 20 ± 1°C. All fluorescence decays have been normalized to the same maximum intensity.

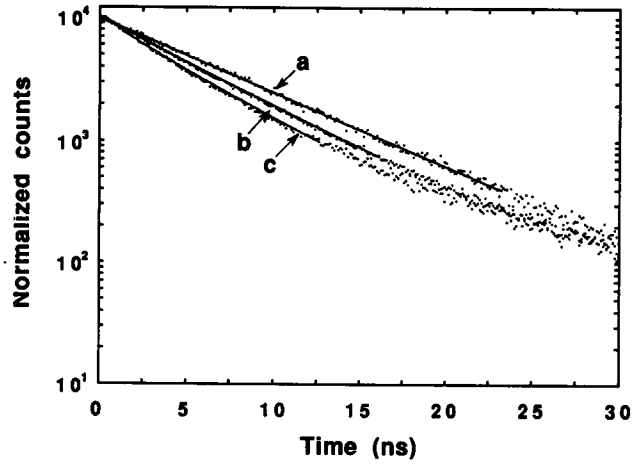

FIGURE 11 Fluorescence decays of a 2 mole % pyrene-DPPE/DPPC monolayer for various concentrations of CAT-16 at 0.97 nm^2 $molecule^{-1}$. (*a*) 0 mole % CAT-16; (*b*) 10 mole % CAT-16; (*c*) 20 mole % CAT-16. All fluorescence decays have been normalized to the same maximum intensity. Subphase: 0.1 M $NaClO_4$. λ_{ex} = 320 nm and λ_{em} = 400 nm. Temperature = 20 ± 1°C.

The lateral diffusion coefficients obtained from the steady-state measurements for the pyrene-DPPE/ODDMA/DMPC system and the pyrene-DPPE/CAT-16/DMPC system are essentially the same. In light of the conclusions that will be drawn from the time-resolved data, this similarity appears to reflect the distortion of the steady-state data by static quenching.

The lateral diffusion coefficients obtained from time-resolved data using CAT-16 as the quencher are somewhat larger than those obtained from time-resolved data for the pyrene-DPPE/ODDMA/DMPC system. The parameter *ha*, which weights reaction against diffusion, extracted from the time-resolved fits using CAT-16 as quencher, yields values greater than 10^3, which suggests that the quenching reaction of pyrene-DPPE by CAT-16 is diffusion controlled (Medhage and Almgren, 1992; Medhage, 1993). This is in agreement with previous monolayer fluorescence quenching experiments (Caruso et al., 1991, 1993b). The lower diffusion coefficients obtained from the time-resolved measurements when ODDMA is used as the quencher may reflect an interaction of ODDMA with the lipid matrix (DMPC) through hydrogen bonding, retarding its motion and leading

to lower values for the diffusion coefficients. The *ha* values also indicated that the quenching of pyrene-DPPE by ODDMA was diffusion controlled. As mentioned earlier, the addition of ODDMA to the monolayer film causes a reduction in the average area per molecule for a particular surface pressure, when compared to the reference monolayer. This introduces some unavoidable uncertainty into the determination of the lateral diffusion coefficients when using ODDMA as quencher.

Since the steady-state measurements are affected by static quenching, only diffusion coefficients obtained from the time-resolved data will be compared to values reported in the literature. The lateral diffusion coefficients measured for the DPPC matrix in the LE phase are about 1–2 $\times$ 10^7 cm^2 s^{-1} (see Table 1). These values are similar to those reported by Peters and Beck (2–3 $\times$ 10^{-7} cm^2 s^{-1}) for the diffusion of *N*-[4-nitrobenz-2,1,3-oxadiazole] egg phosphatidylethanolamine (NBD-egg-PE) in DPPC at the upper surface pressure range of the LE phase, using the FRAP technique (Peters and Beck, 1983). Assuming that the lateral diffusion coefficients of the lipid probe molecules used in the FRAP (NBD-egg-PE) and fluorescence quenching experiments (pyrene-DPPE) are similar, one would expect the lateral diffusion coefficients obtained from FRAP measurements to be smaller than our reported values, since the fluorescence quenching technique gives a mutual diffusion coefficient between the probe and quencher. However, it can be seen from the above comparison that the FRAP values are essentially the same as those extracted from the fluorescence quenching measurements. An explanation for this may be the surface flow caused by minute temperature gradients at the air-water interface present in FRAP measurements (Wu et al., 1977; Kim and Yu, 1992). Such surface flow can interfere with Brownian diffusion and may lead to larger values of the lateral diffusion coefficients.

The lateral diffusion coefficients obtained for the DMPC matrix using CAT-16 as the quencher at 5 mN m^{-1} are (within experimental error) the same as those determined for the DPPC matrix using CAT-16 as the quencher at 3 mN m^{-1} (see Table 1). Both of the monolayers are in the LE phase and occupy about the same average area per molecule (see Fig. 1) at the surface pressures indicated above. The agreement between the lateral diffusion coefficients for these two matrices at about the same average area per molecule suggests that the presence of two additional -CH_2- units in each chain of DPPC does not significantly affect the rate at which pyrene-DPPE and CAT-16 diffuse within the monolayer.

Recently we reported mutual lateral diffusion coefficients ranging from 6 $\times$ 10^{-7} to 2 $\times$ 10^{-7} cm^2 s^{-1} over the surface pressure range of 5 to 35 mN m^{-1} for pyrene-DPPE and CAT-16 in DOPC monolayers (Caruso et al., 1991), using the same fluorescence quenching technique employed in this study. These values are about a factor of 5 larger at low surface pressures and almost an order of magnitude larger at high surface pressures than the diffusion coefficients obtained in this work for the DMPC matrix using CAT-16 as the quencher. Surface pressure-area isotherms reveal that when monolayers of DOPC (di-C_{18}, unsaturated) and DMPC (di-C_{14}, saturated) are in the LE state, there is about a 10–15% difference in the average area per molecule occupied by the lipid molecules at the air-water interface at any given surface pressure (Caruso et al., 1991, 1993a). Although the difference in the average area per molecule is small, there is a major difference in the values of the lateral diffusion coefficients. In order to explain this large difference, lateral diffusion coefficients reported for the analogue fatty acid molecules, myristic acid (C_{14}, saturated), and oleic acid (C_{18}, unsaturated) will be discussed. Using the density fluctuation model of Blank and Britten (1965), Agrawal and Neuman (1988) reported theoretical values ranging from 3.44 $\times$ 10^{-7} cm^2 s^{-1} (at 0.46 nm^2 $molecule^{-1}$) to 0.37 $\times$ 10^{-7} cm^2 s^{-1} (at 0.34 nm^2 $molecule^{-1}$) over the surface pressure range of about 1 to 10 mN m^{-1}, for the lateral self-diffusion coefficients of myristic acid monolayers in the LE phase. These values are in good agreement with results obtained experimentally using radiotracer techniques (Agrawal and Neuman, 1988). Loughran et al. (1980) studied a spread monolayer of 12-(1-pyrenyl)dodecanoic acid in oleic acid at the air-water interface using the pyrene excimer technique. Employing the random walk model and Monte Carlo simulations they estimated a range of 9–17 $\times$ 10^{-7} cm^2 s^{-1} for the lateral diffusion coefficient of 12-(1-pyrenyl)dodecanoic acid. This range agrees well with the theoretical value of 11 $\times$ 10^{-7} cm^2 s^{-1} (at 0.47 nm^2 $molecule^{-1}$) for the lateral self-diffusion coefficient for oleic acid monolayers reported by Agrawal and Neuman (1988). The above results show that lateral diffusion in oleic acid is considerably faster than in myristic acid. Myristic acid and oleic acid differ in chemical structure by four -CH_2- units and the presence of a *cis*-double bond in the acyl chain of oleic acid. It has long been known that the introduction of unsaturation (especially *cis*-double bonds) in molecules can interfere with close packing in air-water monolayers (Gaines, 1966), and this can explain the differences in the lateral diffusion coefficients for myristic acid and oleic acid (see below). Similarly, the large differences in the lateral diffusion coefficients obtained between DOPC and DMPC monolayers clearly demonstrate that the presence of the *cis*-double bond in both the acyl chains of DOPC facilitates lateral diffusion, presumably by reducing the packing density of the lipids in the monolayer compared to DMPC and thus increasing the fluidity.

The difference in the above results may be explained in light of the free area model of Sackmann et al. (Trauble and Sackmann, 1972; Galla et al., 1979), which is the two-dimensional analogue of the free volume model of Cohen and Turnbull (1959). The diffusion coefficient of lipid molecules, modeled as hard rods of cross-sectional area a_o, confined to a cage bounded by immediate neighbors, and moving with local velocity u, is derived as

$$D = gdu \exp(-\gamma a^*/a_f) \quad (7)$$

where g is a geometric factor of the diffusant close to unity, d is approximately the molecular diameter of the diffusant,

γ is a numerical factor between one-half and unity accounting for overlap of the free volume, a^* is the critical free area at which displacement and hence diffusion becomes possible, and a_f is the free area per lipid molecule defined as $a_f = A - a_o$, where A is the average area per molecule. Equation 7 shows that the diffusion coefficient has an exponential dependence on the free area per molecule; that is, small differences in the free area per molecule lead to large changes in the diffusion coefficient. The lateral diffusion coefficients obtained in this study indicate that the DOPC matrix is more fluid than DPPC, which suggests that the free area per molecule for DOPC is larger than that for DPPC. It is therefore plausible that rotational motion of the bent hydrocarbon chains of DOPC is one basic mechanism of creating free volume in unsaturated monolayers.

With regard to the relation between phospholipid bilayers and monolayers, it is relevant to mention the general observations of diffusion of lipid molecules in phospholipid bilayers. In these systems the lateral diffusion coefficients for the lipid molecules have been measured to be on the order of 10^{-8} to 10^{-7} cm^2 s^{-1}. Peters and Beck (1983) obtained a value of $7.7 \pm 0.1 \times 10^{-8}$ cm^2 s^{-1} for the lateral diffusion of NBD-PE in a DLPC bilayer. This value is approximately a factor of 2 smaller than that of 1.5×10^{-7} cm^2 s^{-1} at 38 mN m^{-1}, obtained for the same lipid probe in DLPC monolayers at the same temperature. This suggests that the equivalent pressure of the DLPC bilayer is considerably greater than 38 mN m^{-1} and/or that lateral diffusion in bilayers is "restricted" by additional cohesive forces and/or interdigitation between the hydrocarbon chains in the bilayer. We are currently investigating the hydrocarbon-hydrocarbon chain interactions by using model bilayer systems to determine what influence they have on lateral diffusion in natural bilayers and membranes.

CONCLUSIONS

The fluorescence quenching of a lipoidal pyrene derivative by two amphiphilic quenchers, in air-water monolayers of the phospholipids DMPC and DPPC, has been studied by steady-state and time-resolved methods. The results have been analyzed in the theoretical framework of diffusion-controlled quenching in a two-dimensional environment to yield the mutual lateral diffusion coefficients.

F. C. acknowledges the receipt of a Commonwealth Scientific Industrial Research Organization Institute of Industrial Technologies Research Postgraduate Scholarship for this work. Financial assistance from the Australian Research Council and the Advanced Mineral Products Research Centre (University of Melbourne) is also gratefully acknowledged.

We are most grateful to Dr. E. Mukhtar and Mr. E. Wistus from the Department of Physical Chemistry, University of Uppsala, Uppsala, Sweden, for technical assistance and for helpful discussions.

REFERENCES

Agrawal, M. L., and R. D. Neuman. 1988. Surface diffusion in monomolecular films. II. Experiment and theory. *J. Colloid Interface Sci.* 121: 366–380.

Almeida, P. F. F., W. L. C. Vaz, and T. E. Thompson. 1992. Lateral diffusion in the liquid phases of dimyristoylphosphatidylcholine/cholesterol lipid bilayers: A free volume analysis. *Biochemistry.* 31:6739–6747.

Axelrod, D. 1977. Cell surface heating during fluorescence photobleaching recovery experiments. *Biophys. J.* 18:129–131.

Bevington, P. R. 1969. Data Reduction and Error Analysis for the Physical Sciences. McGraw-Hill, New York.

Birks, J. B. 1970. Photophysics of Aromatic Molecules. Wiley-Interscience, New York.

Blank, M., and J. S. Britten. 1965. Transport properties of condensed monolayers. *J. Colloid Sci.* 20:789–800.

Bohorquez, M., and L. K. Patterson. 1988. Effects of molecular organization on photophysical behaviour. Time-resolved fluorescence of a pyrene-labeled phosphatidylcholine in spread monolayers of dioleoylphosphatidylcholine. *J. Phys. Chem.* 92:1835–1839.

Caruso, F., F. Grieser, A. Murphy, P. J. Thistlethwaite, R. Urquhart, M. Almgren, and E. Wistus. 1991. Determination of lateral diffusion coefficients in air-water monolayers by fluorescence quenching measurements. *J. Am. Chem. Soc.* 113:4838–4843.

Caruso, F., F. Grieser, P. J. Thistlethwaite, M. Almgren, E. Wistus, and E. Mukhtar. 1993a. Behaviour of a pyrene-labelled phospholipid in monolayers of dimyristoyl-L-α-phosphatidylcholine at the gas-water interface. A fluorescence quenching study. *J. Phys. Chem.* 97:7364–7370.

Caruso, F., F. Grieser, P. J. Thistlethwaite, and M. Almgren. 1993b. Lateral diffusion of amphiphiles in fatty acid monolayers at the air-water interface: a steady-state and time-resolved fluorescence quenching study. *Langmuir.* In press.

Chapman, D. 1993. Biomembranes and new hemocompatible materials. *Langmuir.* 9:39–45.

Cherry, R. J. 1979. Rotational and lateral diffusion of membrane proteins. *Biochim. Biophys. Acta.* 559:289–327.

Cohen, M. H., and D. Turnbull. 1959. Molecular transport in liquids and glasses. *J. Chem. Phys.* 31:1164–1169.

Devaux, P., and H. M. McConnell. 1972. Lateral diffusion in spin-labeled phosphatidylcholine multibilayers. *J. Am. Chem. Soc.* 94:4475–4481.

Dörfler, H-D. 1990. Mixing behaviour of binary insoluble phospholipid monolayers. Analysis of the mixing properties of binary lecithin and cephalin systems by application of several surface and spreading techniques. *Adv. Colloid Interface Sci.* 31:1–110.

Edidin, M. 1974. Rotational and translational diffusion in membranes. *Annu. Rev. Biophys. Bioeng.* 3:179–201.

Espenson, J. H. 1981. Chemical Kinetics and Reaction Mechanisms. McGraw-Hill, Inc., New York. 169.

Gaines, G. L. 1966. Insoluble Monolayers at Liquid-Gas Interfaces. Wiley-Interscience, New York. 233.

Galla, H-J., and E. Sackmann. 1974a. Lateral mobility of pyrene in model membranes of phospholipids with different chain lengths. *Ber. Bunsen-Ges. Phys. Chem.* 78:949–953.

Galla, H-J., and E. Sackmann. 1974b. Lateral diffusion in the hydrophobic region of membranes: Use of pyrene excimers as optical probes. *Biochim. Biophys. Acta.* 339:103–115.

Galla, H. J., W. Hartmann, U. Theilen, and E. Sackmann. 1979. On two-dimensional passive random walk in lipid bilayers and fluid pathways in biomembranes. *J. Membr. Biol.* 48:215–236.

Hackenbrock, C. R. 1981. Lateral diffusion and electron transfer in the mitochrondrial inner membrane. *Trends Biochem. Sci.* 6:151–154.

Heimenz, P. C. 1977. Principles of Colloid and Surface Chemistry. Marcel Dekker, Inc., New York and Basel. 210.

Kano, K., H. Kawazumi, T. Ogawa, and J. Sunamoto. 1981. Fluorescence quenching in liposomal membranes. Exciplex as a probe for investigating artificial lipid membrane properties. *J. Phys. Chem.* 85:2204–2209.

Kim, S., and H. Yu. 1992. Lateral diffusion of amphiphiles and macromolecules at the air/water interface. *J. Phys. Chem.* 96:4034–4040.

Lösche, M., E. Sackmann, and H. Möhwald. 1983. A fluorescence microscopic study concerning the phase diagram of phospholipids. *Ber. Bunsen-Ges. Phys. Chem.* 87:848–852.

Loughran, T., M. D. Hatlee, L. K. Patterson, and J. Kozak. 1980. Monomer-excimer dynamics in spread monolayers. I. Lateral diffusion of pyrene dodecanoic acid at the air-water interface. *J. Chem. Phys.* 72:5791–5797.

Medhage, B. 1993. Fluorescence dynamics studies of microheterogeneous

systems. Ph.D. thesis, Uppsala University, Uppsala, Sweden.

Medhage, B., and M. Almgren. 1992. Diffusion-influenced fluorescence quenching dynamics in one to three dimensions. *J. Fluorescence*. 2:7–21.

Meller, P. 1988. Computer-assisted video microscopy for the investigation of monolayers on liquid and solid substrates. *Rev. Sci. Instrumen.* 59: 2225–2231.

Meller, P., R. Peters, and H. Ringsdorf. 1989. Microstructure and lateral diffusion in monolayers of polymerizable amphiphiles. *Colloid Polym. Sci.* 267:97–107.

Miller, D. D., and D. F. Evans. 1989. Fluorescence quenching in double-chained surfactants. 1. Theory of quenching in micelles and vesicles. *J. Phys. Chem.* 93:323- 333.

O'Connor, D. V., and D. Phillips. 1984. Time-Correlated Single Photon Counting. Academic, London.

Owen, C. S. 1975. Two dimensional diffusion theory: cylindrical diffusion model applied to fluorescence quenching. *J. Chem. Phys.* 62:3204–3207.

Peters, R. 1981. Translational diffusion in the plasma membrane of single cells as studied by fluorescence microphotolysis. *Cell Biol. Int. Rep.* 5:733–760.

Peters, R., and K. Beck. 1983. Translational diffusion in phospholipid monolayers measured by fluorescence microphotolysis. *Proc. Natl. Acad. Sci. USA.* 80:7183- 7187.

Scandella, C. J., P. Devaux, and H. M. McConnell. 1972. Rapid lateral diffusion of phospholipids in rabbit sarcoplasmic reticulum. *Proc. Natl. Acad. Sci. USA.* 69:2056- 2060.

Smith, B. A., and H. M. McConnell. 1978. Determination of molecular motion in membranes using periodic pattern photobleaching. *Proc. Natl. Acad. Sci. USA.* 75:2759–2763.

Smith, L. M., R. M. Weis, and H. M. McConnell. 1981. Measurement of rotational motion in membranes using fluorescence recovery after photobleaching. *Biophys. J.* 36:73–91.

Stroeve, P., and I. Miller. 1975. Lateral diffusion of cholesterol in monolayers. *Biochim. Biophys. Acta.* 401:157–167.

Subramanian, R., and L. K. Patterson. 1985. Effects of molecular organization on photophysical behaviour. Excimer kinetics and diffusion of 1-pyrene-decanoic acid in lipid monolayers at the nitrogen-water interface. *J. Am. Chem. Soc.* 107:5820–5821.

Tamm, L. K., and H. M. McConnell. 1985. Supported phospholipid bilayers. *Biophys. J.* 47:105–113.

Teissie, J., J-F. Tocanne, and A. Baudras. 1978. A fluorescence approach of the determination of translational diffusion coefficients of lipids in phospholipid monolayer at the air-water interface. *Eur. J. Biochem.* 83: 77–85.

Trauble, H., and E. Sackmann. 1972. Studies of crystalline-liquid crystalline phase transition of lipid model membranes. III. Structure of a steroid-lecithin system below and above the lipid-phase transition. *J. Am. Chem. Soc.* 94:4499–4510.

Urquhart, R., F. Grieser, P. J. Thistlethwaite, E. Wistus, M. Almgren, and E. Mukhtar. 1992. Steady-state and time-resolved study of two-dimensional Förster energy transfer between 4-heptadecyl-7-hydroxycoumarin and RhB-DPPE in phospholipid air-water monolayers. *J. Phys. Chem.* 96:7808–7816.

Vanderkooi, J. M., S. Fischkoff, M. Andrich, F. Podo, and C. S. Owen. 1975. Diffusion in two dimensions: comparison between diffusional fluorescence quenching in phospholipid vesicles and in isotropic solution. *J. Chem. Phys.* 63:3661–3666.

Weber, G. 1966. Flavins and Flavoproteins. E. C. Slater, editor. Elsevier, Amsterdam. 15.

Wistus, E., E. Mukhtar, M. Almgren, and S-E. Lindquist. 1992. Behavior of pyrene in air/water monolayers of eicosanoic acid. *Langmuir.* 8: 1366–1371.

Wu, E-S., K. Jacobson, and D. Papahajopoulos. 1977. Lateral diffusion in phospholipid multibilayers measured by fluorescence recovery after photobleaching. *Biochemistry.* 16:3936–3941.